Journal of Engineering Physics and Thermophysics, Vol. 79, No. 5, 2006

HYDROGASDYNAMICS IN TECHNOLOGICAL PROCESSES

TALBOT INTERFEROMETRY IN MEASUREMENTS OF THE PARAMETERS OF AN AXISYMMETRIC TURBULENT JET

M. V. Doroshko,[a] O. G. Penyaz'kov,[a] G. Rankin,[b] K. L. Sevruk,[a] P. P. Khramtsov,[a] and I. A. Shikh[a]

UDC 532.517.4

The Talbot effect has been adapted to measurement of the parameters of mixing in an axisymmetric turbulent helium jet flowing out into a submerged air space. A two-dimensional array of angles of refraction of light has been determined from the displacement of the image of unit Talbot elements in the reproduction plane of the time-averaged talbogram. The distribution of the average refractive index of a medium and the concentration of helium in the flow field have been calculated by means of the Abel transformation. Based on an analysis of the intensity distribution at the maxima of the Talbot image, it has been shown that the turbulence of this jet is locally inhomogeneous and anisotropic.

Reproduction of the intensity distribution of the field of coherent monochromatic radiation with a periodically modulated front, which is known as the Talbot effect [1], is quite frequently used for diagnostics of different objects. In particular, the moiré technique, where the object under study is placed between two identical exposed gratings and both the size and type of inhomogeneity are evaluated by the distortion of the resulting moiré pattern [2, 3], is constructed on this principle. Casnerale et al. [4, 5] have proposed a scheme (called the Talbot interferometer) in which the receiving grating is placed in the reproduction plane of the first grating, which enables one to increase the base and sensitivity of measurements. In [6–12], the Talbot-interferometer scheme has been used for achromatic light.

In a number of investigations [13–16], the Talbot effect has been successfully used for diagnostics of the quality of laser-active media, including flowing gas lasers. Since the range of possible amplitudes and scales of inhomogeneities in gas flows is fairly wide, the technique for measuring them must possess the corresponding accuracy, dynamic range, and resolution. Talbot interferometry entirely meets these requirements in view of the high sensitivity of the technique to a change in the local angles of refraction of light. Two components of the deflection angle can simultaneously be established at any point of a phase object with a high space density, which is determined by the period of a Talbot grating. Furthermore, recording of an ordered interference pattern in the reproduction plane offers a number of advantages compared to the techniques on the basis of random-interference effects [17, 18] due to the much higher sensitivity of the Talbot image (talbogram) to phase distortions and due to its resolution and contrast. This enables one to substantially simplify the procedure of processing of a talbogram and to improve the measurement accuracy.

Methods of monitoring optical distortions based on the Talbot effect continue to actively be developed [19–26] for different engineering and scientific applications. Below, we demonstrate certain capabilities of Talbot interferometry in measuring the average and pulsation characteristics of turbulent flows. The flow structure occurring when an axisymmetric turbulent helium jet flows out into a submerged air space has been selected as the object.

Measurement of the Turbulence Parameters Using Talbot Interferometry. The use of the Talbot effect for diagnostics of turbulent media possesses a number of features related to the presence of disorder of the flow, in which

[a]A. V. Luikov Heat and Mass Transfer Institute, National Academy of Sciences of Belarus, 15 P. Brovka Str., Minsk, 220072, Belarus; [b]Fluid-Dynamics Research Institute, University of Windsor, Canada. Translated from Inzhenerno-Fizicheskii Zhurnal, Vol. 79, No. 5, pp. 94–99, September–October, 2006. Original article submitted May 20, 2005.

1062-0125/06/7905-0937

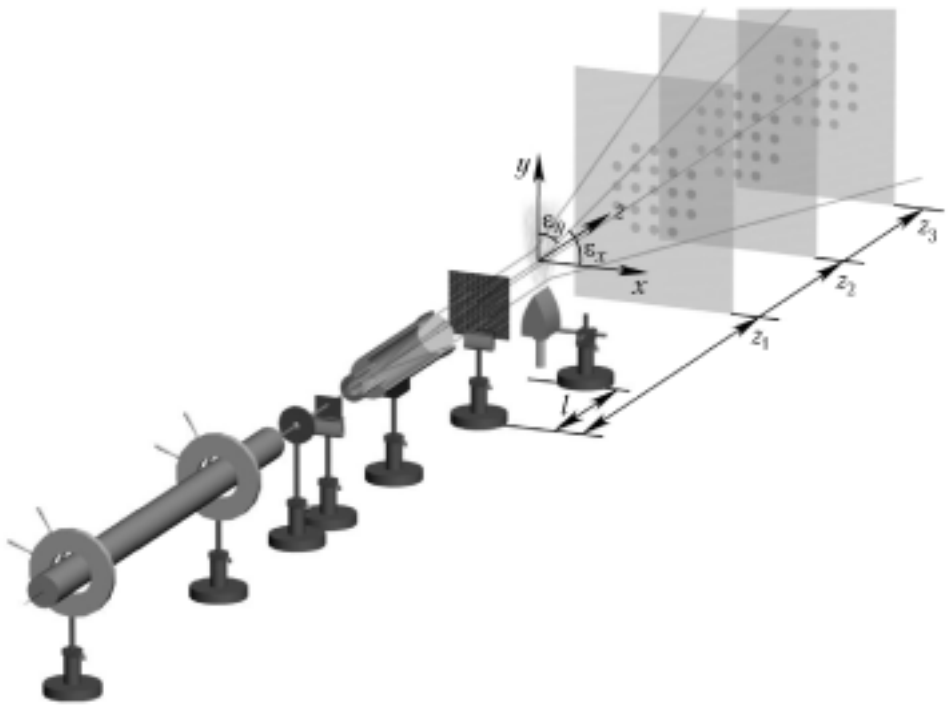

Fig. 1. Optical scheme of the experimental setup for investigation of the statistical characteristics of turbulent flows using the Talbot effect.

the quantities characterizing the flow experience random changes along the time and space coordinates. An analogous behavior is also characteristic of the optical flow parameters. The instantaneous (recorded using Talbot interferometry) value of the local angle of deflection of light in the case of turbulent flow can be considered as the sum of the average (over time) and pulsation values

$$\varepsilon(x, y, t) = \overline{\varepsilon(x, y)} + \varepsilon'(x, y, t), \quad \bar{\varepsilon} = \lim_{T\to\infty} \frac{1}{2T} \int_{-T}^{+T} \varepsilon dt . \tag{1}$$

On the time-averaged talbogram, the displacement of unit intensity maxima or elements of the talbogram from their initial position leads to a blurring of the image, which is caused by the pulsations of the gradient of the refractive index in the flow. The range of displacement of the center of gravity of a unit element is related to the average value of the local refraction angle, whereas the light-intensity distribution within the unit element depends on the spectral pulsation density related to the standard value of the pulsations of the deflection angle $\overline{(\varepsilon')^2}(x, y)$ by the relations

$$\int_0^\infty E_{\varepsilon_x}(k)\, dk = \overline{(\varepsilon'_x)^2}, \quad \int_0^\infty E_{\varepsilon_y}(k)\, dk = \overline{(\varepsilon'_y)^2}. \tag{2}$$

An optical scheme of the experimental setup for investigation of the statistical characteristics of turbulent flows with the use of Talbot interferometry is presented in Fig. 1. The radiation of an He–Ne laser is converted, upon transmission by the aperture diaphragm and the neutral filter, to a homogeneous wide-aperture light beam with an approximately plane wave front using the collimator. The Talbot grating, representing a thin film with a system of uniformly distributed orthogonally packed holes, is fixed between a pair of plane-parallel plates of high optical quality and is placed in the region of the laser beam immediately behind the collimator. A system forming turbulent flow of the type under study (nozzle, gas burner, etc.) is installed at a certain distance from the grating (no larger than z_1). Depending on the required sensitivity of the technique, a screen is placed in the plane of reproduction of the tal-

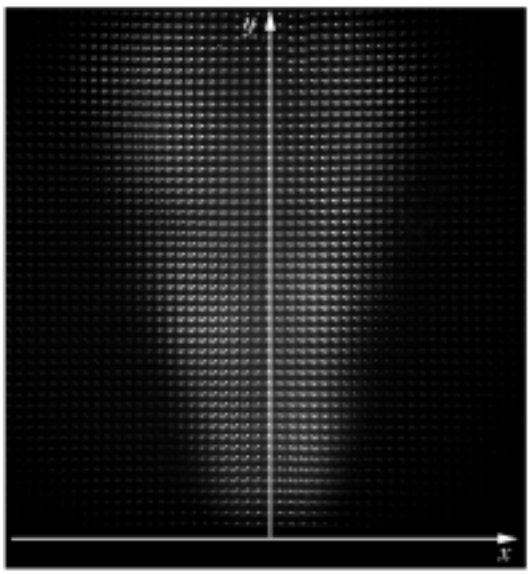

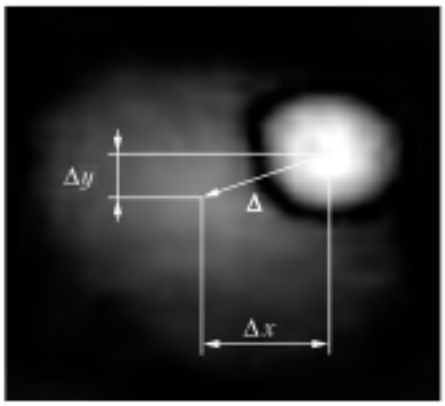

Fig. 2. Talbogram of an axisymmetric helium jet. The exposure time is 1 sec.

Fig. 3. Intensity distributions in a unit element of the talbogram before and after the transmission of light by an axisymmetric turbulent jet.

bogram at a distance z_N from the grating surface. The length z_N determines the position of reproduction planes in which the field distribution replicates the distribution on the grating, i.e., $z_N = 2p^2N/\lambda$. The image on the screen replicating the initial distribution of the incident-light intensity is recorded with a required space and time resolution using a high-quality digital camera.

An axisymmetric helium jet was used in the work as the object of investigation. The jet was formed in flowing out of the gas via a circular nozzle installed immediately behind the Talbot grating at a small distance l (Fig. 1). The diameter of the nozzle exit section structurally located at the base of the confuser part of a cylindrical channel (equipped with a system of honeycombs) was $3\cdot10^{-3}$ m. The nozzle was supplied with the gas via a receiver in which a constant pressure was maintained. The flow velocity in the nozzle exit section was maintained constant during the experiments and was ≈40 m/sec.

The density of the neutral filter and the entrance aperture of the lens of a Canon 300D digital camera were selected so as to obtain the optimum quantity of light on the photorecording matrix of a charge-coupled device (CCD) in exposures sufficient for averaging of turbulent pulsations. The difference flow pattern produced in the reproduction plane is presented in Fig. 2. It is seen that, in addition to the local displacement of the intensity maxima over the flow field $\Delta_i = (\Delta X_i, \Delta Y_i)$, which are caused by the presence of the average angles of refraction of light, we have their substantial smearing due to turbulent pulsations. Figure 3 gives the intensity distributions in a unit element of the talbogram before and after the transmission of light by the axisymmetric turbulent jet. It is seen that the pulsation component of the local deflection angle substantially transforms the character of the intensity distribution in the unit element, which has an approximately elliptic shape with values of the ratios of large and small semiaxes and the angle of their inclination to the x axis different over the flow field of the jet. As is seen from expressions (2), the noncircular shape of unit elements of the Talbot image and the inclinations of large semiaxes of the ellipses demonstrate the inhomogeneity and anisotropy of the field of turbulent pulsations in jet flow.

Calculation of the Distribution of the Average Concentration of Helium in the Field of Axisymmetric-Jet Flow from the Average Talbogram. Since the axis of symmetry of the turbulent jet was perpendicular to the optical axis of the setup in measurements and was directed along the x axis, the Euler equations for the angles of deflection of light in a cylindrical coordinate system can be transformed to the Abel equations

$$\varepsilon_x = \frac{2}{n_0}\int_y^R \frac{\partial n}{\partial r}\frac{y}{\sqrt{r^2-y^2}}\,dr\,, \quad \varepsilon_y = \frac{2}{n_0}\int_y^R \frac{\partial n}{\partial x}\frac{y}{\sqrt{r^2-y^2}}\,dr\,. \tag{3}$$

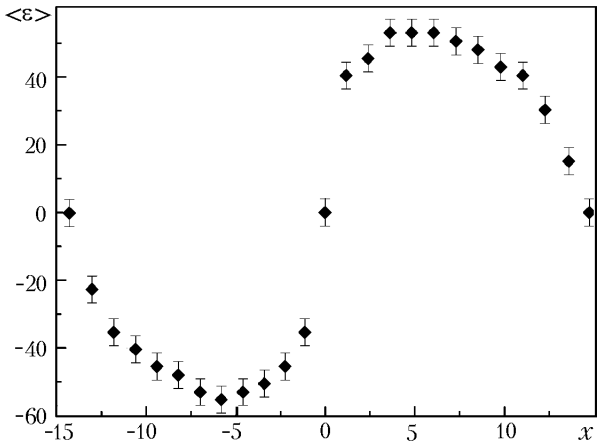

Fig. 4. Distribution of the average angle of deflection of light at the distance from the nozzle exit section $y = 10\ D$. $\langle\varepsilon\rangle$, angular seconds; x, mm.

Figure 4 gives the characteristic form of the distribution of the average angle of deflection of light for one cross section of the axisymmetric jet.

To transform the Abel integral to a form resolved for the function $n(r)$ determined [27], multiplying Eq. (3) by $1/\sqrt{y^2 - r^2}$ and integrating with respect to y^2, after simple transformations we obtain

$$\frac{1}{r}\frac{\partial n}{\partial r} = \frac{1}{\pi}\left[\frac{\varepsilon_y(R)/y}{\sqrt{R^2 - r^2}} - \int_r^R \frac{\partial}{\partial y}\left(\frac{\varepsilon_y(y)}{y}\right)\frac{dy}{\sqrt{y^2 - r^2}}\right], \quad \frac{\partial n}{\partial x} = \frac{1}{\pi}\left[\frac{\varepsilon_x(R)}{\sqrt{R^2 - r^2}} - \int_r^R \frac{\partial \varepsilon_x(y)/\partial y}{\sqrt{y^2 - r^2}}\,dy\right]. \tag{4}$$

Since the light beam transmitted by an inhomogeneity at the point $y = R$ is not deflected, Eqs. (4) can be written in the form

$$\frac{1}{r}\frac{\partial n}{\partial r} = -\frac{1}{\pi}\int_r^R \frac{\partial}{\partial y}\left(\frac{\varepsilon_y(y)}{y}\right)\frac{dy}{\sqrt{y^2 - r^2}}, \quad \frac{\partial n}{\partial x} = -\frac{1}{\pi}\int_r^R \frac{\partial \varepsilon_x(y)/\partial y}{\sqrt{y^2 - r^2}}\,dy. \tag{5}$$

By repeated integration of the first equation of (5), we find

$$\frac{n - n_0}{n_0} = -\frac{1}{\pi}\int_r^R \frac{\varepsilon_y(y)}{\sqrt{y^2 - r^2}}\,dy. \tag{6}$$

In diagnostics of turbulent flows with Talbot interferometry, use is made of a discrete set of data on the average flow parameters (Fig. 4) dependent on the period of a Talbot grating p, so that relation (6) can be written in recurrence form:

$$\overline{n(r_i)} = n_0 - \frac{n_0}{\pi}\sum_{k=i}^{M} \frac{\varepsilon_y(y_k)\,\Delta y_k}{\sqrt{y_k^2 - r_i^2}}. \tag{7}$$

The distribution of the refractive index of the medium in the turbulent jet which has been restored in such a manner can be used for calculation of the average concentration of helium in the flow field. Considering a helium—air mixture as a binary one and assuming that the values of the refractive index for gas media differ from unity only slightly, we represent the Lorentz–Lorenz formulas in the form of the system of equations

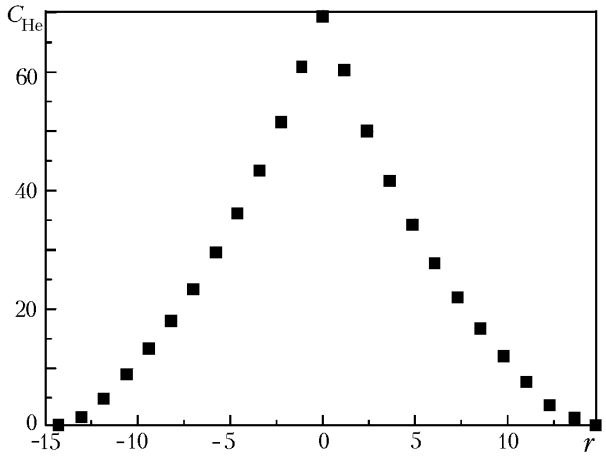

Fig. 5. Distribution of the average concentration of helium at the distance from the nozzle exit section $y = 10\ D$. r, mm.

$$\overline{n-1} = 2\pi\,(\overline{N}_1 a_1 + \overline{N}_2 a_2)\,, \tag{8}$$

where $\overline{N}_1 + \overline{N}_2 = \overline{N}$. The results of calculations of the average concentration of helium in the field of jet flow from formulas (7) and (8) on the basis of the data of Fig. 4 are presented in Fig. 5.

It is obvious that the characteristic features of flow occurring in interaction and dissipation of jets of heterogeneous gases can be revealed in the distributions of the concentration of helium and the average angle of deflection of light. The possibility of measuring the spatial distribution of the average concentration of the impurity makes this technique quite promising when the processes of turbulent mixing are studied.

The investigations carried out enable us to infer that Talbot interferometry is a powerful means for diagnosing liquid or gas flows, including turbulent ones. The technique allows determination of a two-dimensional array of local angles of refraction of light with a high spatial resolution (step to 200 μm) over the flow field and a sensitivity to 10^{-5} rad comparable to the sensitivity of high-quality shadow units of the type IAB-451. The optical scheme of the technique is easy to implement, requires no expensive optical elements, and is clear and easy to operate. Owing to the small number of elements, including a periodically transmitting Talbot grating and a collimator, the technique depends on external disturbances only slightly and can be used under industrial conditions.

The applied capabilities of the technique have been illustrated by its use for measurement of such average parameters of an axisymmetric turbulent helium jet flowing out into a submerged air space as the refractive-index distribution and the concentration of helium in the flow field.

This work was carried out with support from the Foundation for Basic Research of the Republic of Belarus (project No. T03MF-046).

NOTATION

a_1 and a_2, polarization factors of helium and air molecules respectively, m^3; C_{He}, concentration of He, %; D, nozzle diameter, m; E_{ε_x} and E_{ε_y}, spectral density of pulsations of the local deflection angle, $rad^2 \cdot m$; k, wave number, m^{-1}; l, distance from the Talbot grating to the object under study, m; M, number of unit Talbot elements in the field of jet flow; n, refractive index; N_1 and N_2, concentrations of the components of the mixture, m^{-3}; p, period of the Talbot grating, mm; r, running radius in the cylindrical coordinate system, m; R, jet radius, m; t, running time, sec; T, averaging period, sec; x, y, and z, running Cartesian coordinates, m; z_1, z_2, and z_3, distances to Talbot images of the corresponding orders, m; $\boldsymbol{\Delta}_i$, radius vector of displacement of a unit Talbot element from the initial position, m; λ, incident-radiation wavelength, μm; ε, ε_x, and ε_y, local angles of deflection of light, rad. Subscripts and superscripts: i, running index; k, order of restoration of a Talbot image; x, y, coordinates in the cross-sectional plane of the jet; 0, undisturbed medium; ′, pulsation component of the medium's parameters; ¯, time averaging.

REFERENCES

1. F. Talbot, Facts relating to optical science, IV, *Philos. Mag.*, **9**, 401–407 (1836).
2. J. Ebbeni, Nouveaux aspects du phenomene de moiré, *Nouv. Rev. Opt.*, **1**, No. 5, 333–342 (1970).
3. Y. Nakono and K. Mwata, Measurements of phase objects using the Talbot effect and moiré techniques, *Appl. Opt.*, **23**, 2296–2299 (1984).
4. M. Casnerale and B. Daino, Application of the Talbot interferometer, *Opt. Acta*, **24**, 1099 (1977).
5. C. S. Lim and V. Srinivasun, Talbot interferometer with computer generated gratings, *Opt. Commun.*, **44**, No. 3, 219–222 (1983).
6. E. Lau, Beugungserscheinungen an Doppelrastern, *Ann. Phys.*, Bd. 6, 417–423 (1948).
7. A. W. Lohmann and D. E. Silva, An interferometer based on the Talbot effect, *Opt. Commun.*, **2**, No. 9, 413–415 (1971).
8. M. L. Roblin, Realisation d'un systeme des franges a chromatiques a pas variable, *Opt. Acta*, **18**, 539–545 (1971).
9. N. O. Bartelt and J. Jahns, Interferometry based on the Lau effect, *Opt. Commun.*, **30**, No. 4 (1979).
10. S. Yokozeki and T. Suzuki, Shearing interferometer using the grating as the beam splitter, *Appl. Opt.*, **10**, 1575–1580 (1971).
11. D. Silva, A simple interferometric method of beam collimation, *Appl. Opt.*, **10**, 1980–1982 (1971).
12. V. Ronchi, Forty years of history of a grating interferometer, *Appl. Opt.*, **3**, 437–451 (1964).
13. A. S. Koryakovskii and V. M. Marchenko, *On the Effect of Optical Inhomogeneities on Reproduction of Periodic Distributions of a Coherent Field and the Mode of an Optical Cavity of a Flow-Through Generator* [in Russian], Preprint No. 89 of the Physical Institute of the Academy of Sciences, Moscow (1979).
14. A. S. Koryakovskii and V. M. Marchenko, Interferometry of optical inhomogeneities of active media of Talbot-effect-based lasers, *Kvantovaya Élektron.*, **7**, No. 5, 1048–1057 (1980).
15. A. S. Koryakovskii and V. M. Marchenko, The wave-front pickup based on the Talbot effect, *Zh. Tekh. Fiz.*, **51**, No. 6, 1432–1438 (1981).
16. A. S. Koryakovskii, V. M. Marchenko, and A. M. Prokhorov, The diffraction theory of the Talbot-interferometry method and diagnostics of wide-aperture wave fronts, *Tr. IOFAN*, **7**, 33–91 (1987).
17. U. Wernekinck, W. Merzkich, and N. Fomin, Measurement of light deflection in a turbulent density field, *Exp. Fluids*, No. 3, 208–215 (1985).
18. N. Fomin, *Speckle Photography for Fluid Mechanics Measurements*, Springer-Verlag, Berlin (1998).
19. N. Saiga and Y. Ichioka, Visualization of the strain wave front of a progressive acoustic wave based on the Talbot effect, *Appl. Opt.*, **24**, 1459–1465 (1985).
20. D. Joyeux and Y. Cohen-Sabban, High magnification self-imaging, *Appl. Opt.*, **21**, 625–627 (1982).
21. C. Shakher and A. K. Anil Kumar Nirala, A review on refractive index and temperature profile measurements using laser-based interferometric techniques, *Optics Lasers Eng.*, **31**, 455–491 (1999).
22. G. S. Spagnolo, D. Ambrosini, and D. Paoletti, Displacement measurement using the Talbot effect with a Ronchi grating, *J. Opt. A: Pure Appl. Opt.*, **4**, 376–380 (2002).
23. A. M. Andreyev, V. M. Ginzburg, and N. M. Ramishvili, The use of the Talbot effect in dynamic measurements of deformed liquid/gas interface surface shape, *Opt. Commun.*, **73**, No. 6, 429u433 (1989).
24. Zhang Qi-Can and Su Xian-Yu, An optical measurement of vortex shape at a free surface, *Optics Laser Technol.*, **34**, No. 2, 107–113 (2002).
25. W. Yu and D. Yun, Talbot and Fourier moiré deflectometry and its applications in engineering evaluation, *Optics Lasers Eng.*, **25**, 163–177 (1996).
26. J. Stricker and B. Zakharin, 3-D turbulent density field diagnostics by tomographic moiré technique, *Exp. Fluids*, **23**, No. 1, 76–85 (1997).
27. M. M. Skotnikov, *Quantitative Shadow Methods in Gas Dynamics* [in Russian], Nauka, Moscow (1976).